Highly compression-tolerant folded carbon nanotube/paper as solid-state supercapacitor electrode

Yu Song[1], Xiaoliang Cheng[1], Haotian Chen[2], Mengdi Han[1], Xuexian Chen[2], Jiahuan Huang[1], Zongming Su[1], Haixia Zhang[1,2] ✉

[1]*National Key Laboratory of Science and Technology on Micro/Nano Fabrication, Institute of Microelectronics, Peking University, Beijing 100871, People's Republic of China*
[2]*Academy for Advanced Interdisciplinary Studies, Peking University, Beijing 100871, People's Republic of China*
✉ *E-mail: zhang-alice@pku.edu.cn*

Published in Micro & Nano Letters; Received on 5th May 2016; Accepted on 28th June 2016

An original highly compression-tolerant folded carbon nanotube (CNT)/paper electrode, which could be assembled into compressible solid-state supercapacitor with polyvinyl alcohol/phosphoric acid gel electrolyte, is designed. It is worth mentioning that both the compression-tolerant ability of the folded structure and the strain ability of the CNT electrode are conducive to achieving the compressible supercapacitor. Such device could withstand pressure and shape-changing, which has great potential to be used in various environments. This compressible solid-state supercapacitor also owns the maximum specific capacitance of 11.07 mF/cm^2, and capacitance retention retains more than 90% after 100 cycling times. Furthermore, the stability performance of the device is also discussed which is almost steady under 50% strain state. When two devices are connected in serial and fully charged, this power unit could light up a red light emitting diode continuously even under the compression state. Therefore, this device performs as a promising candidate to be compatible with other compression-tolerant electronics and enlightens a broad field of compressible energy storage and self-powered systems.

1. Introduction: With the rapid development of consumer electronics as well as advances in wearable devices [1], harvesting mechanical energy from the environment is widely considered an attractive approach [2]. Considerable efforts have been devoted to developing sustainable energy, such as triboelectric nanogenerators [3, 4], piezoelectric nanogenerators [5, 6] and solar cell [7, 8]. Besides various energy harvesters, high-performance energy storage devices [9], as another critical component in self-powered system [10], are in great demand.

Supercapacitor, as a promising state-of-the-art energy storage device, bridges the gap between the batteries with high specific energy density and the conventional electrostatic capacitors with high specific power density [11, 12]. Solid-state supercapacitors integrating electrodes, solid-state electrolyte and separator [13, 14], are superior to the liquid-based supercapacitor [15] due to easy fabrication, light-weight, high safety and compatibility with environment. Meanwhile, electronic devices with highly deformation-tolerant ability have attracted tremendous attention [16, 17]. They can easily maintain the desired levels of performance and reliability due to their flexibility of integration into various forms systems [18, 19]. As a crucial component of electronics system, power source devices should definitely have the ability to withstand large strains and own long-term stability in various environments.

However, there has been limited progress in developing supercapacitors which could withstand pressure and shape changing. Recent demonstrations have shown that graphene [20], carbon nanotubes (CNTs) [21] and their composite sponge [22] can serve as compressible electrodes, which can be assembled into the supercapacitor with a complicated figuration. However, sponge electrode is easy to tear, suffering from the low stability in mechanical manufacture. On the other hand, sponge is not suitable for many electronic device, which could extremely limit its application.

Therefore, considering the fact that paper is the cheapest substrate and easily integrated with other devices, such as microfluidics systems [23] and radio frequency device [24], and CNTs could be efficiently absorbed in the paper, such CNT/paper electrode owns high conductivity and excellent mechanical strength [25]. Besides, the folded structure is available to own highly compression-tolerant ability. The compressible solid-state supercapacitor is innovatively assembled with such electrode and gel electrolyte, which can solve the mentioned problems and make great progress in flexible electronics and wearable devices.

2. Experimental procedure: As shown in Fig. 1, it shows the compressible solid-state supercapacitor based on the folded structure. The optical image of the device is demonstrated in Fig. 1*a*, which owns the uniformly folded structure and excellently mechanical strength. The total dimension of the device is 4, 2.5 and 0.7 cm, respectively. In addition, the schematic illustration of proposed compressible solid-state supercapacitor is shown in Fig. 1*b*, which is composed of three parts: the flexible folded CNT/paper electrode, solid-state polyvinyl alcohol (PVA)/phosphoric acid (H_3PO_4) electrolyte and the separator membrane.

The detailed fabrication process is illustrated in Fig. 2. First, two pieces of filter paper and a cellulose membrane (TF44, NKK, Japan) as a separator film with an area of 16 cm^2 were both folded as wavy shape. Second, CNT ink solution was prepared by dispersing 60 mg of CNTs with 60 mg of sodium dodecylbenzenesulfonate surfactant in 60 ml of deionised water. After the CNT ink solution was bath-sonicated for 4 h to disperse evenly, approximately 30 ml CNT ink was drop-dried on each folded paper for several times until CNT was saturated and dried at 80°C for 1 h in an oven.

Then PVA/H_3PO_4 electrolyte was prepared by adding PVA powder (6 g) into H_3PO_4 aqueous solution (6 g H_3PO_4 into 60 ml deionised water). The whole mixture was heated to 85°C under vigorous stirring until the solution became clear. After cooling down, two folded CNT/paper electrodes were immersed into the solid-state PVA/H_3PO_4 electrolyte for 5 min and then all of them were assembled into a symmetrical supercapacitor by sandwiching the separator between them. Finally, the device was dried in a regular oven at 45°C for about 12 h to fully vaporise the excess water.

The morphologies, structure of the compressible CNT/paper electrode and the assembled supercapacitor were all analysed using a

doi: 10.1049/mnl.2016.0255

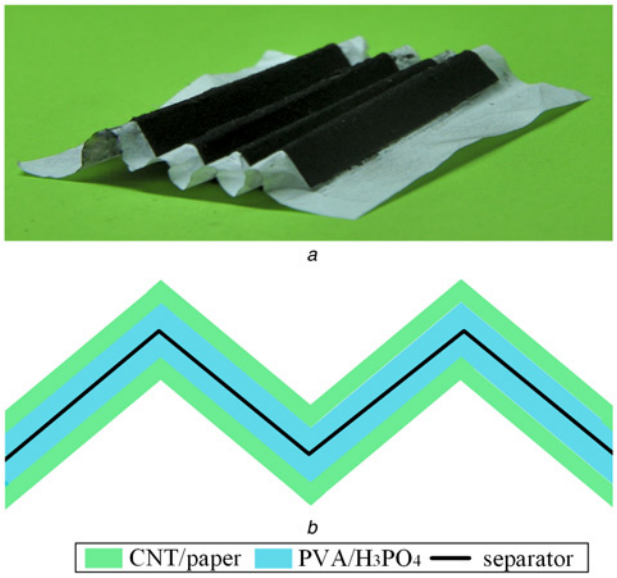

Fig. 1 *Compressible solid-state supercapacitor based on folded structure*
a Optical image of compressible supercapacitor
b Schematic illustration of compressible sueprcapacitor

scanning electron microscope (SEM) (Quanta 600F, FEI Co.). For the relatively electrochemical measurement of the compressible solid-state supercapacitor, an electrochemical workstation (CHI660) was utilised by using cyclic voltammetry (CV) and galvanostatic charge–discharge (GCD) techniques with a two-electrode configuration at room temperature.

3. SEM image analysis: The flexible and conductive paper electrodes was simply fabricated by drop-drying CNT ink solution onto the paper. Fig. 3*a* illustrates the SEM image of the proposed paper, which was uniformly coated with CNTs, showing the capability to be a conductive electrode. Furthermore, Fig. 3*b* presents the cross-sectional SEM image of the sandwiched structure of the compressible supercapacitor, which owns great symmetrical ability.

4. Compressible stability of electrode: As for electrode stability, the resistance of CNT/paper electrode is almost steady in the first 200 compressing-releasing process cycles, showing the excellently compression-tolerant ability (Fig. 4). Therefore, this electrode could be potentially used in highly compressible

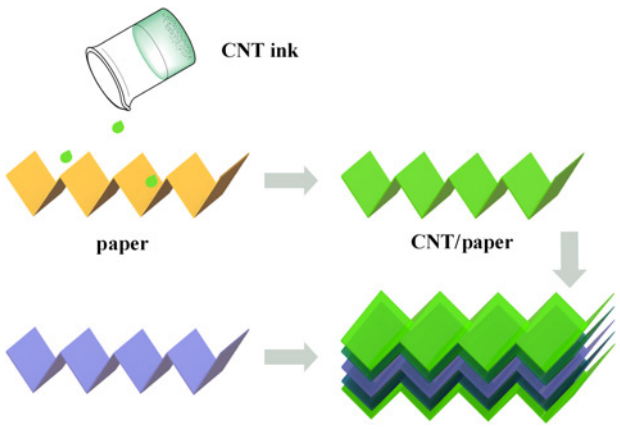

Fig. 2 *Experimental procedure to fabricate compressible supercapacitor consisting of folded CNT/paper electrode, PVA/H_3PO_4 electrolyte and NKK TF44 separator membrane*

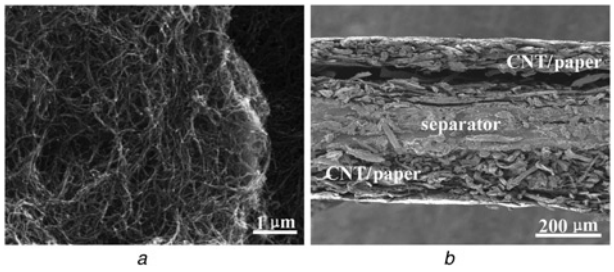

Fig. 3 *SEM image of the compressible supercapacitor*
a Top view of the CNT/paper electrode
b Cross-section view of the sandwiched structure

solid-state supercapacitor, without either an insulating binder or a low capacitance conducting additive.

5. Compressible test of supercapacitor: With the gel electrolyte, the folded electrodes could be further assembled into an integral compressible device. The compression-tolerant ability is performed where the device is operated under different

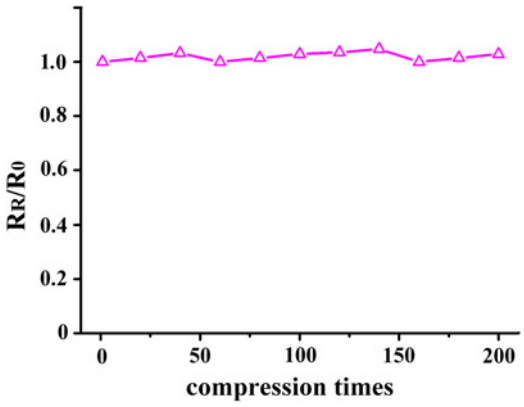

Fig. 4 *Variation of the electrical resistance of CNT/paper electrode in the first 200 compressing-releasing cycles*

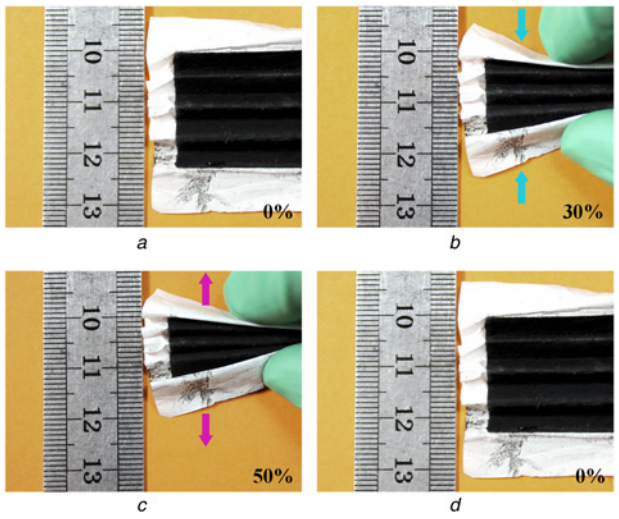

Fig. 5 *Real-time optical image of compressible supercapacitor under different strain state*
a Under initial state
b Under 30% strain state
c Under 50% strain state
b Recovery to initial state without any structural damage

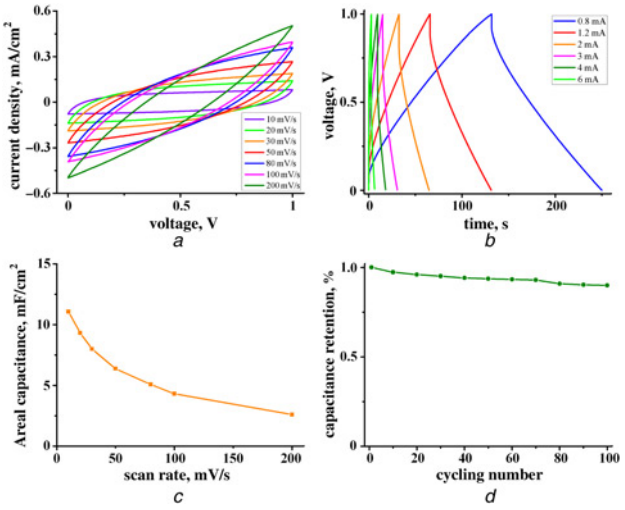

Fig. 6 *Electrochemical behaviour of the compressible supercapacitor*
a CV curves at different scan rates
b GCD curves at different charging–discharging currents
c Areal capacitance calculated through CV curves
d Capacitance cycling stability test at scan rate of 100 mV/s

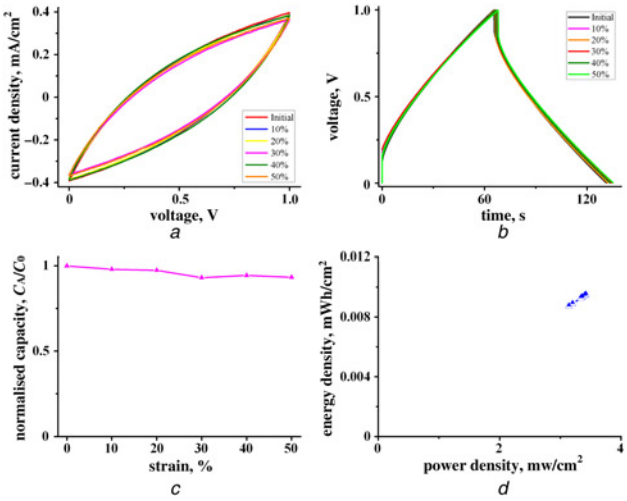

Fig. 7 *Electrochemical behaviour of compressible supercapacitor under different strain states*
a CV curves at the scan rate of 100 mV/s
b GCD curves at the charging–discharging current of 1.2 mA
c Normalised specific capacitance through CV curves
d Ragone plot of the compressible supercapacitor

compression states from initial state to more than 50% strain state. As shown in Figs. 5*a*–*d*, the device can sustain large-strain deformations under manual compression and recover to the initial state without any observable structural crack. In addition, this device could restore most of lengths after several repeated compressing-releasing cycles.

6. Electrochemical analysis: To further explore the electrochemical performance of the compressible supercapacitor, the area of which is 16 cm^2, several measurements are carefully analysed including CV, GCD and cycling stability measurements via an electrochemical workstation with two-electrode configuration.

First, electrochemical performance is tested by CV curves at scan rates from 10 to 200 mV/s. As shown in Fig. 6*a*, the CV curves retain quasi-rectangular shape and are approximately symmetrical about the zero-current line, indicating an ideal electrochemical behaviour.

Then GCD curve is also analysed to further evaluate the electrochemical performance of solid-state supercapacitor. Typical GCD curves are demonstrated in Fig. 6*b*, the charging–discharging currents of which are from 0.8 to 6 mA. The charging profile of the device is dependent on the applied current and similar curve shapes have been obtained under different charging–discharging currents. It is obvious that all of the charging curves are also symmetrical with their corresponding discharging counterparts, as well as their excellent linear voltage-time profiles, showing the fast charge–discharge abilities of the device.

Besides, the areal capacitance (C_A) is calculated through the CV curves of the supercapacitor achieved by the following equations

$$C = \frac{Q}{\Delta V} = \frac{1}{k \cdot \Delta V}\int_{V_1}^{V_2} I(V)\mathrm{d}V \tag{1}$$

$$C_A = \frac{C}{A} = \frac{1}{k \cdot A \cdot \Delta V}\int_{V_1}^{V_2} I(V)\mathrm{d}V \tag{2}$$

where C is the total capacitance, $I(V)$ is the discharge current function, k is the scan rate, ΔV is the potential window during the discharge process and A is the area of the supercapacitor. The maximum C_A is 11.07 mF/cm^2 at scan rate of 10 mV/s and C_A decreases slightly with the scan rate increasing (Fig. 6*c*), demonstrating a relatively good electrochemical capability. In addition, the specific capacitance cycling stability performance of the device is also measured shown in Fig. 6*d*. The fabricated solid-state supercapacitor shows long-term cycling stability after 100 charge–discharge cycling times, and the specific capacitance retains more than 90% compared with the initial state.

As a compressible supercapacitor, the relationship between the strain and the electrochemical performance is also a significant evaluation. When such compressible supercapacitor is applied different strains from initial state to 50% strain state, no obvious change is observed in the CV curves at the voltage scan rate of 100 mV/s and GCD curves at the charging–discharging current of 1.2 mA, respectively, thus indicating the electrochemical stability performance of the device (Figs. 7*a* and *b*). Besides, the normalised capacitance of the compressible supercapacitor is also calculated through (2) and discussed in Fig. 7*c*. It can be found that the specific capacitance of the device is nearly not altered and maintains more than 90% under the 50% strain state.

The Ragone plot showing the energy density with respect to the power density of fabricated solid-state supercapacitor at initial state is presented in Fig. 7*d* at different voltage scan rates. The energy density and power density of the device could be calculated by the following equations

$$E = \frac{1}{2}C_A(\Delta V)^2 \tag{3}$$

$$P = \frac{3600E}{\Delta t} \tag{4}$$

where C_A is the areal capacitance of the supercapacitor which can be achieved through (2), ΔV is also the potential window during discharging process, and Δt is the discharging time. The highest energy density of the compressible supercapacitor is 0.0095 mWh/cm^2 at the scan rate of 10 mV/s, at the same time, the highest power density is 3.42 mW/cm^2 at the scan rate of 200 mV/s, respectively. Definitely, both of them vary slightly with the increase of the applied strain.

7. Applications: When two such compressible supercapacitor is serially connected and fully charged, this power unit could be powerful enough to light up red light emitting diode (LED) continuously as shown in Fig. 8*a*. Furthermore, this unit would

doi: 10.1049/mnl.2016.0255

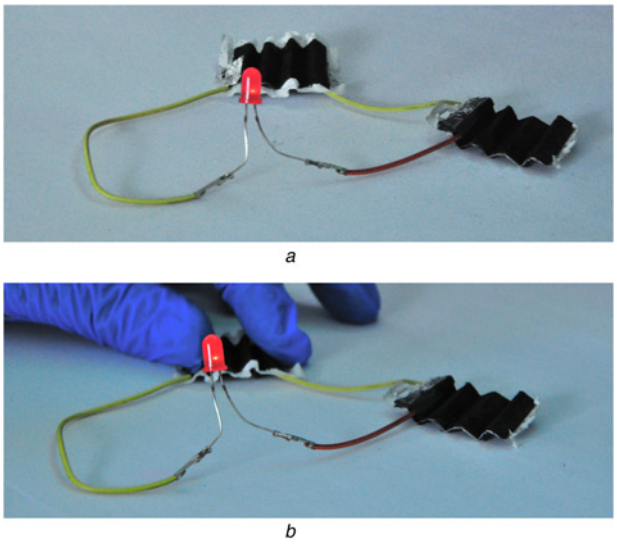

Fig. 8 *LED lit by a power unit composed of two compressible supercapacitors serially connected*
a Optical image of such power unit
b Stably work under compressed state

work stably even when it is under compressed and subsequently recovered to the initial state (Fig. 8*b*). Therefore, such device can be further integrated with other power unit and have excellent advantages in the compression-tolerant applications.

8. Optimisation: To further improve the compressible performance of the device, optimisation of the structure is a good option. To study the relationship between the pressure applied on the device and the strain distribution, we conduct the finite element simulation (COMSOL) to compare the two different structure. As shown in Fig. 9*a*, the folded structure with sharp bending is faced with the problems where the device is easy to break at the bending position. Then with the optimisation of arc bending (Fig. 9*b*), the strain decreases dramatically at the bending position, which could enhance the compression-tolerant ability. Furthermore, with the same pressure applied, the device with arc bending owns smaller deformation than the device with sharp bending, which accounts for the fact that the device with arc bending could withstand greater pressure and be more stable than the former device.

9. Conclusion: In summary, we fabricated compressible CNT/paper electrodes by simply 'drop-drying' process with folded structure, the resistance of which is steady under the repeated compressing-releasing cycles. This steady CNT/paper electrode performs a promising candidate in compression-tolerant devices. Then such electrode could be assembled into the highly compressible solid-state supercapacitor with the PVA/H_3PO_4 gel electrolyte. With this unique configuration, the whole device could be compressed as an integrated unit, which is able to fully recover to the initial state without any structural damage under several compressing-releasing cycles. The specific capacitance of this compressible supercapacitor reaches 11.07 mF/cm^2 at the scan rate of 10 mV/s, and capacitance retention retains more than 90% after 100 charge–discharge cycling times, thus showing long-term stability. In addition, the performance of the compressible supercapacitor is relatively stable and maintains more than 90% under the different applied strains from initial state to more than 50% strain state. When two such devices are serially connected and fully charged, the unit could drive a LED continuously even under compressed state. More importantly, with the optimisation of the structure, hybrid electrodes and integration with nanogenerators, such device has plenty of room to be enhanced. Therefore, with the highly compression-tolerant electrode, such supercapacitor provides a marvellous power storage choice for the advanced applications of wearable devices and mechanical systems.

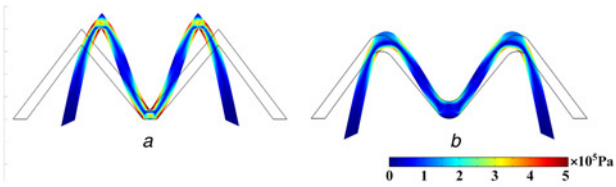

Fig. 9 *Finite element simulation results of the relationship between strain distribution and the bending structure*
a Strain distribution of the sharp bending structure
b Strain distribution of the optimised arc bending structure

10. Acknowledgments: This work was supported by the National Natural Science Foundation of China (grant nos. 61176103, 91023045 and 91323304), the National Hi-Tech Research and Development Program of China ('863' Project) (grant no. 2013AA041102), and the Beijing Science & Technology Project (grant no. Z141100003814003) and the Beijing Natural Science Foundation of China (grant no. 4141002).

11 References

[1] Meng B., Cheng X., Zhang X., *ET AL.*: 'Single-friction-surface triboelectric generator with human body conduit', *Appl. Phys. Lett.*, **2014**, 104, p. 103904
[2] Mitcheson P.D., Yeatman E.M., Rao G.K., *ET AL.*: 'Energy harvesting from human and machine motion for wireless electronic devices', *Proc. IEEE*, 2008, **96**, pp. 1457–1486
[3] Zhang X., Han M., Meng B., *ET AL.*: 'High performance triboelectric nanogenerators based on large-scale mass-fabrication technologies', *Nano Energy*, 2015, **11**, pp. 304–322
[4] Wang Z.L.: 'Triboelectric nanogenerators as new energy technology for self-powered systems and as active mechanical and chemical sensors', *ACS Nano*, 2013, **7**, pp. 9533–9557
[5] Wang Z.L., Song J.: 'Piezoelectric nanogenerators based on zinc oxide nanowire arrays', *Science*, 2006, **312**, pp. 242–246
[6] Han M.D., Zhang X.S., Meng B., *ET AL.*: 'r-Shaped hybrid nanogenerator with enhanced piezoelectricity', *ACS Nano*, 2013, **7**, pp. 8554–8560
[7] O'regan B., Grfitzeli M.: 'A low-cost, high-efficiency solar cell based on dye-sensitized', *Nature*, 1991, **353**, pp. 737–740
[8] Mailoa J.P., Bailie C.D., Johlin E.C., *ET AL.*: 'A 2-terminal perovskite/silicon multijunction solar cell enabled by a silicon tunnel junction', *Appl. Phys. Lett.*, 2015, **106**, p. 121105
[9] Xiao X., Zhou W., Kim Y., *ET AL.*: 'Regulated breathing effect of silicon negative electrode for dramatically enhanced performance of Li-Ion battery', *Adv. Funct. Mater.*, 2015, **25**, pp. 1426–1433
[10] Wang J., Wen Z., Zi Y., *ET AL.*: 'All-plastic-materials based self-charging power system composed of triboelectric nanogenerators and supercapacitors', *Adv. Funct. Mater.*, 2016, **26**, pp. 1070–1076
[11] Simon P., Gogotsi Y.: 'Materials for electrochemical capacitors', *Nature Mater.*, 2008, **7**, pp. 845–854
[12] Miller J., Simon P.: 'Electrochemical capacitors for energy management', *Science*, 2008, **321**, pp. 651–652
[13] Xiao X., Li T., Yang P., *ET AL.*: 'Fiber-based all-solid-state flexible supercapacitors for self-powered systems', *ACS Nano*, 2012, **6**, pp. 9200–9206
[14] Song Y., Meng B., Chen X.X., *ET AL.*: 'Fabrication and characterization analysis of flexible porous nitrogen-doped carbon-based supercapacitor electrodes (in Chinese)', *Chin. Sci. Bull.*, 2016, **61**, pp. 1314–1322
[15] Sathyamoorthi S., Suryanarayanan V., Velayutham D.: 'Organo-redox shuttle promoted protic ionic liquid electrolyte for supercapacitor', *J. Power Sources*, 2015, **274**, pp. 1135–1139
[16] Hu H., Zhao Z., Wan W., *ET AL.*: 'Ultralight and highly compressible graphene aerogels', *Adv. Mater.*, 2013, **25**, pp. 2219–2223
[17] Li Y., Chen J., Huang L., *ET AL.*: 'Highly compressible macro-porous graphene monoliths via an improved hydrothermal process', *Adv. Mater.*, 2014, **26**, pp. 4789–4793

[18] Zhang X., Han M., Wang R., *ET AL.*: 'Frequency-multiplication high-output triboelectric nanogenerator for sustainably powering biomedical microsystems', *Nano Lett.*, 2013, **13**, pp. 1168–1172
[19] Cheng X., Meng B., Zhang X., *ET AL.*: 'Wearable electrode-free triboelectric generator for harvesting biomechanical energy', *Nano Energy*, 2015, **12**, pp. 19–25
[20] Zhao Y., Liu J., Hu Y., *ET AL.*: 'Highly compression-tolerant supercapacitor based on polypyrrole-mediated graphene foam electrodes', *Adv. Mater.*, 2013, **25**, pp. 591–595
[21] Niu Z., Zhou W., Chen X., *ET AL.*: 'Highly compressible and all-solid-state supercapacitors based on nanostructured composite sponge', *Adv. Mater.*, 2015, **27**, pp. 6002–6008
[22] Zhang Y., Zhen Z., Zhang Z., *ET AL.*: 'In-situ synthesis of carbon nanotube/graphene composite sponge and its application as compressible supercapacitor electrode', *Electrochim. Acta*, 2015, **157**, pp. 134–141
[23] Niedl R., Beta C.: 'Hydrogel-driven paper-based microfluidics', *Lab Chip*, 2015, **15**, pp. 2452–2459
[24] Subramanian V., Fréchet J., Chang P., *ET AL.*: 'Progress toward development of all-printed RFID tags: materials, processes, and devices', *Proc. IEEE*, 2005, **93**, pp. 1330–1338
[25] Kang Y.J., Chung H., Han C.H., *ET AL.*: 'All-solid-state flexible supercapacitors based on papers coated with carbon nanotubes and ionic-liquid-based gel electrolytes', *Nanotechnology*, 2012, **23**, pp. 65401–65406

doi: 10.1049/mnl.2016.0255